Journal of Advanced Research (2014) 5, 79–86

Cairo University

Journal of Advanced Research

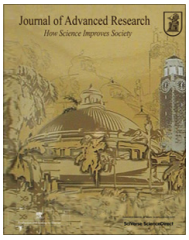

ORIGINAL ARTICLE

Effect of ethylene carbonate as a plasticizer on CuI/PVA nanocomposite: Structure, optical and electrical properties

Shaimaa A. Mohamed [a,*], A.A. Al-Ghamdi [b], G.D. Sharma [c], M.K. El Mansy [d]

[a] *Center for Photonic and Smart Materials (CPSM), Zewail City of Science and Technology, Sheikh Zayed District, 6th of October City, 12588, Giza, Egypt*
[b] *Physics Department, Faculty of Science, King Abdulaziz University, Jeddah 21589, Saudi Arabia*
[c] *R & D Center for Engineering and Science, Jaipur Engineering College, Kukas, Jaipur (Raj.) 303 101, India*
[d] *Department of Physics, Faculty of Science, Benha University, Benha, Egypt*

ARTICLE INFO

Article history:
Received 25 August 2012
Received in revised form 28 November 2012
Accepted 30 November 2012
Available online 11 January 2013

Keywords:
CuI/PVA polymer composite
Electrical characterization
Optical band gap
Bulk conductivity

ABSTRACT

Layers of ethylene carbonate (EC) modified CuI/PVA polymer composites were prepared by growth of CuI nano-particles in an aqueous solution of PVA followed by casting at room temperature. The structural, thermal, optical, electrical and di-electrical characterization of polymer composites was investigated using different techniques. These investigations confirm the growth of CuI nano-particles and reduction of PVA crystallinity by increasing ethylene carbonate concentration. These results show that energy band gap and bulk conductivity increase while activation energy reduces with the increase of EC concentration in the composite. Moreover, the variation of the dielectric permittivity and dielectric loss with EC content are found to obey Debye dispersion relations.

Introduction

The production of electricity from sunlight is an attractive renewable source for clean energy. Traditional photovoltaic cells are made from high expensive materials such as silicon which require high purity and expensive processing techniques. Great efforts have been focused on the developments of solar cells that can scale up to large area with low cost of fabrication. Recent trends are directed to thin film devices of photoactive layers which consists of conjugated polymer as an organic part (donor) and semiconductor nano-crystalline as inorganic part (acceptor). These devices are called hybrid organic–inorganic solar cells, and they are arranged in two different structures, the bilayer and the bulk heterojunction (BHJ). In the BHJ, donor and acceptor materials are blended together and deposited onto a substrate to form the active

* Corresponding author. Tel.: +20 1061653973.
E-mail address: dr.shaimaa0206@hotmail.com (S.A. Mohamed).
Peer review under responsibility of Cairo University.

Production and hosting by Elsevier

2090-1232 © 2014 Cairo University. Production and hosting by Elsevier B.V. All rights reserved.
http://dx.doi.org/10.1016/j.jare.2012.11.008

layer [1–5]. The unique properties of inorganic semiconductor nanoparticles with properties of organic/polymeric materials are combined in these types of devices. In addition, they are characterized by low cost and versatile fabrication technique making them attractive. Furthermore, inorganic semiconductor nanoparticles may have high absorption coefficients, and particle size induced tuning of the optical band-gap. Thus, the organic/inorganic hybrid concept for photovoltaic solar cells is getting interesting and attractive in recent years [6–9]. Among these nanoparticles CuI (copper iodide) is a *p*-type high band gap material of ~3.1 eV which belong to *I–VII* semiconductor and exhibit promising results when employed as a hole conducting material for dye sensitized solar cells [10–12]. It exists in three crystalline phase of α, β, and γ. The α phase is a cubic structure at temperature of 392 °C while the hexagonal β-phase is an ionic conductor with temperature between 392 °C and 350 °C. The γ-phase appears at temperature below 350 °C and behaves as *p*-type semiconductor with zinc blende cubic structure [13]. The coordination chemistry of CuI makes it readily coupled with many inorganic and organic ligands. Therefore, CuI materials have a wide range of applications in electronic devices such as light-emitting diodes, liquid–crystal displays, photovoltaic devices, photo-thermal collectors and so on.

The use of polymers is a prominent method for the synthesis of semiconductor nanoparticles [14,15]. The reason is that the polymer matrices enable process ability due to solubility, and control the growth and morphology of the nanoparticles. In this regards, PVA is a potential material having high dielectric strength, good charge storage capacity, and its electrical and optical properties depends on the dopant. It contains carbon chain backbone with hydroxyl groups attached to methane carbons. These OH groups can be a source of hydrogen bonding and hence assist in the formation of polymer blends [16,17].

One way to improve ionic conductivity is to incorporate nano-size oxide fillers such as TiO_2, ZrO_2, and SiO_2, or add low molecular weight organic plasticizers like ethylene carbonate (EC) (melting = 36 °C). The incorporation of plasticizer yield polymer electrolyte with enhanced conductivity by reducing crystallinity but with poor mechanical properties. Also, the addition of low molecular weight and high dielectric constant plasticizer such as ethylene carbonate (EC) enhance the amorphous phase of the polymer and increase the flexibility and release of mobile charge carriers due to ion dissolution effect [18]. Besides, plasticizer increases volume within the electrolyte system and decreases the viscosity of the electrolyte making the mobility of ions became easier [19].

It was reported that, the PVA/CuI polymer materials have been studied as an electron donor in photovoltaic junctions because of their efficient absorption in solar energy spectra [20–22]. Although, solar energy conversion efficiency is greatly influenced by exciton generation, diffusion, dissociation, and electron hole transportation in polymer composite matrix. However, the electrical conduction and dielectric parameters play an important role in solar energy conversion. Therefore, we aim in this work to modify both optical and electrical properties of CuI/PVA composites by using different content of EC so they can be used as an active layer for solar cells.

Material and methods

Polyvinyl alcohol polymer (PVA) used in the present study was provided by Sigma–Aldrich (code CAS 9002-89-5, Batch#:039K0147) while other chemicals were provided by QualiKems Chemical Company, India. A PVA solution was prepared by adding the de-ionized distilled water to solid PVA $(-C_2H_4O)_n$ (where n = 30,000–70,000 average molecular weight) and then stirred on the magnetic stirrer at room temperature, 30 °C, for 2 h. After aging the solution for another 1 h, a solution of $CuCl_2$ in H_2O was added into the PVA under constant stirring and then the proper weight of NaI dissolved in water was added for 2 h drop wise into the reaction vessel to get polymer nano-composite with 10 wt.% of CuI. EC was added to the mixture and complete dissolution was obtained using a magnetic stirrer for another 2 h. The as-prepared composite solution was then uniformly spread in glass Petri dishes and left to dry for 48 h at room temperature 30 °C and used for the further investigations. The thicknesses of the films are around 0.4 mm.

In order to investigate the structure of the polymer electrolyte layers, X-ray diffraction patterns were carried out using Philips X'Pert X-ray diffractometer, Netherlands, using the Cu Kα radiation (λ = 1.540 Å) in a range of 2θ = 5–70°. DSC studies were carried out using (Shimadzu DSC-50) thermal analyzer, USA, from room temperature and up to 350 °C in an aluminum seal under nitrogen atmosphere with flow rate of 30 ml/min. and heating rate of 20 °C/min. Variation of melting point and glass transition temperature with change of ethylene carbonate content was recorded and studied. The optical absorption of the polymer composite colloidal was measured in the wavelength range 190–1100 nm using JENWAY 6405 UV–visible spectrophotometer, Lithuania, at room temperature. The morphology of the sample surface was observed using JEOL scanning electron microscope model JEM-100S, USA. Samples are placed on Cu holder and then coated with gold using JEOL ion sputter unit model (JFC 100E). The size of nanoparticles was determined by analyzing the SEM images using adope photoshop analysis program. The both sides layer of polymer nano-composite were coated with silver paint on the desired area and used for conductivity measurements. Electrical measurements were carried out in the temperature range 303–373 K using PM 6304 programmable automatic RCL (Philips) meter, United States, in the frequency range 0.1–100 kHz.

Results and discussion

X-ray diffraction

Fig. 1a–e represent the diffraction pattern for polymer nanocomposite 10 wt.% CuI/PVA with different EC content of 0, 2.5, 5, 7.5 and 10 wt.% respectively. It is obvious that the broad peak located at 2θ = 19.12° is related to the PVA as reported elsewhere [23–25]. The apparent reduction of PVA characteristic peak height with increasing EC plasticizer can be attributed to the polymer plasticization which leads to polymer chains separation followed by the structure rearrangement. This in turns results in a decrease of the degree of

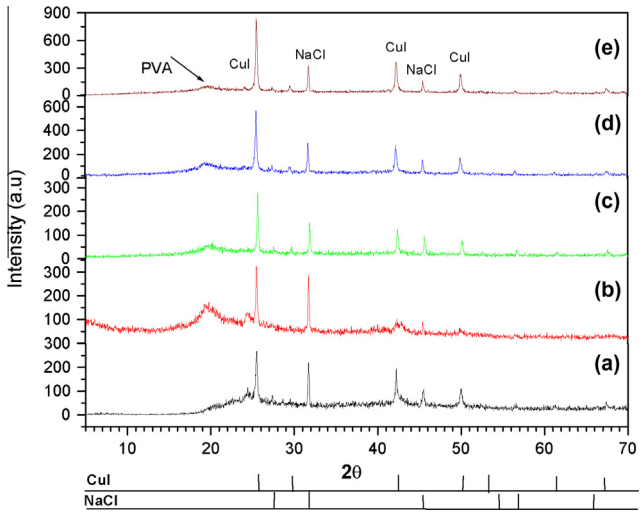

Fig. 1 X-ray diffraction pattern for 10 wt.% CuI/PVA polymer composite blended with different concentrations of EC; (a) 0 wt.%, (b) 2.5 wt.%, (c) 5 wt.%, (d) 7.5 wt.%, and (e) 10 wt.%.

crystallization of PVA. Other peaks observed at $2\theta = 25.5°$, 27.5°, 42.24°, 49.99° and 61.17° reflect the presence of CuI nano-crystals [20–22]. The observed increase of the CuI characteristic peak height at $2\theta = 25.5°$ with increasing EC refers to the increase of ordering CuI nanocrystals in the clusters of nanostructure. Furthermore, sharp peaks are detected at $2\theta = 31.7°$ and 45.4° which refer to the presence of NaCl crystallites and their peak height decrease by increasing EC concentration. The average particle size of CuI nanocrystals has been calculated according to the first sphere approximation of Debye–Scherrer formula [25];

$$D = \frac{0.9\lambda}{B\cos\theta} \quad (1)$$

where D is the average diameter of the crystals, λ is the wavelength of X-ray radiation, B is the full width at half maximum intensity of the peak (FWHM). The obtained particle size of CuI embedded in polymer composite matrix for the different concentration of EC lies in the range of 38.5–67.5 nm as listed in Table 1. It can be noticed that, as the concentration of EC increases up to 5 wt.%, a remarkable increase of the CuI nanoparticles size is observed, whereas it is nearly unchanged beyond such concentration. This can be explained as follow: at the lower concentration of EC up to 5 wt.% the plasticization of polymer composite matrix took place and led to reduction of polymer matrix viscosity and subsequently CuI nanoparticles adherent with polymer structure network. This in turns results in the attraction and clustering of CuI nanoparticles with an apparent increase of particle size beyond 5 wt.% of EC and hence the little fluctuation observed of CuI particle size is due to the competition of nanoparticles clustering and nanocluster dissociation.

Scanning electron microscope investigation

The scanning electron microscope (SEM) technique has been used to investigate the morphology of the sample surfaces and the compatibility between various components of the polymer nanocomposites through the detection of phase separations and interfaces. It has great influence on the physical properties of the polymer nanocomposite. Fig. 2a–d shows the SEM micrographs of the polymer composite PVA/10% CuI blended with different concentrations of EC i.e. 2.5–10 wt.%. The texture of polymer composite matrix consists of large domains with clear boundaries covered with nano-particles in the range 11–32 nm are clearly observed which are less than those estimated from X-ray diffraction peaks. This can be attributed to the presence of NaCl nano-particles with smaller particle sizes, besides CuI nano-particles. The recorded change of morphology as shown in Fig. 2a–d, can be explained as follows: the blending of CuI/PVA polymer composite with EC, in general, results in the dissolution of the of polymer composite, i.e. polymer chain separation by EC plasticizer molecules which reduces their self-adherent. This will facilitate the movement and diffusion of polymer chains at domain boundaries which results in surface roughness reduction and increment of matrix domains area at 5 wt.% of EC (as seen in Fig. 2b). By further increase of EC beyond 5 wt.%, the polymer composite matrix fragmentations took place and results in reduction of domain areas and surface roughness at the higher EC concentrations 7.5 and 10 wt.%.

DSC thermal analysis

Deferential scanning thermogram for Pure PVA polymer was previously studied [26,27]. The DSC investigation of 10 wt.% CuI/PVA polymer composite with different concentrations of EC revealed two essential transition temperatures, i.e. melting (T_m) and glass transition (T_g) temperatures as shown in Fig. 3. It can be seen from this figure that the glass transition temperature lies in the temperature range between 175.9 °C and 180.7 °C while the melting temperature fluctuates in the range 238–251 °C for all EC concentrations except 10 wt.% where T_m shifts to 306.2 °C. The value of enthalpy ΔH for the glass

Table 1 The obtained data of CuI XRD peak height, particle size, activation energy, exponent s and the optical band gap for CuI/PVA-EC polymer composites.

EC content (wt.%)	CuI XRD peak height	D (nm)	E_b (eV)	s	E_g (eV)
0	225.7	38.5	0.79	0.58	1.7
2.5	264.2	41.5	0.97	0.63	2.01
5	278	67.5	0.55	0.29	2.06
7.5	513	53.9	0.45	0.62	2.13
10	799.5	61.3	0.21	0.47	2.18

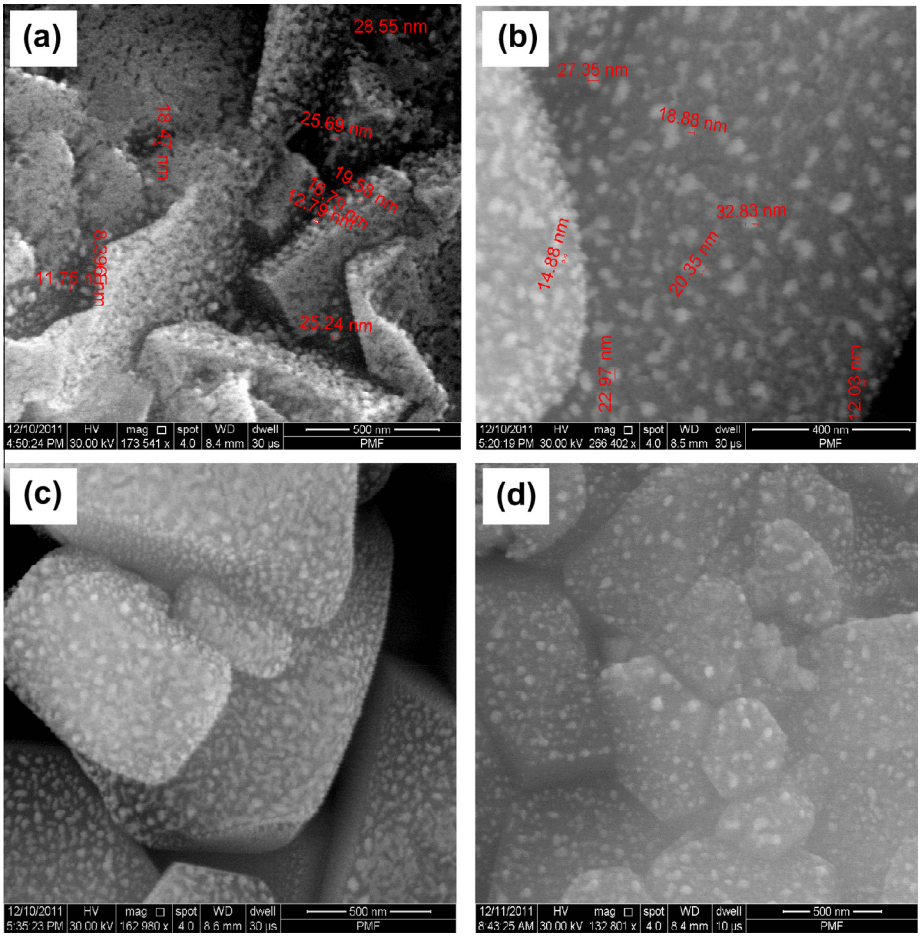

Fig. 2 SEM images for 10 wt.% CuI/PVA polymer composite blended with different Concentrations of EC; (a) 2.5 wt.%, (b) 5 wt.%, (c) 7.5 wt.%, and (d) 10 wt.%.

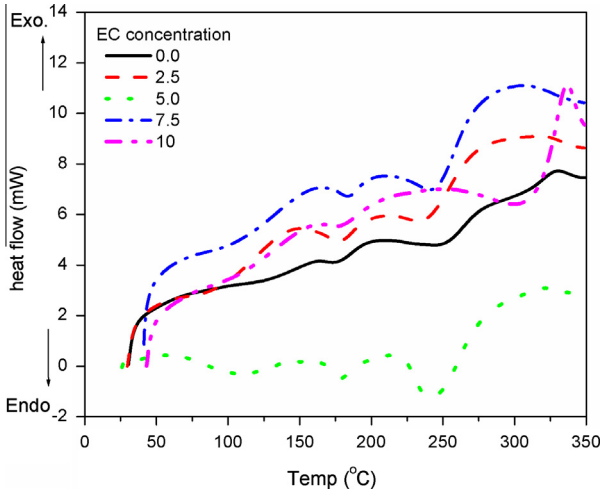

Fig. 3 DSC thermograms for 10 wt.% CuI/PVA polymer composite blended with different concentrations of EC.

transition temperature is −9.17 (J/g) for the composite without EC reach to −31.5 (J/g) at 2.5 wt.% EC then starts to decrease at 5 wt.% EC. The melting temperature enthalpy also illustrates the gradual increase up to 5 wt.% and beyond that its value shows an abrupt decrease at 7.5 wt.% followed by an increase at 10 wt.% as shown in Table 2.

Table 2 Extracted values of T_g, T_m, enthalpies, dielectric constant and dielectric loss of 10% CuI/PVA polymer composite with different concentration of EC.

EC (wt.%)	0	2.5	5	7.5	10
T_g (°C)	175.9	178	179	185.4	180.7
ΔH_g (J/g)	−9.17	−31.5	−25.8	−14.3	−14.29
T_m (°C)	251.3	238.8	241.2	244.1	306.2
ΔH_m (J/g)	−54.6	−66.74	−143.9	−98.19	−246.4
$\varepsilon' \times 10^{-2}$	4.1	13.4	33.5	15.8	9.4
$\varepsilon'' \times 10^{-3}$	2.3	1.5	7.4	0.33	2.4

UV–visible optical absorption

The optical absorption spectrum is an important tool to obtain the energy band gap of crystalline and amorphous materials. The fundamental absorption, which corresponds to the electron excitation from the valance band to the conduction band, can be used to determine the nature and value of the energy

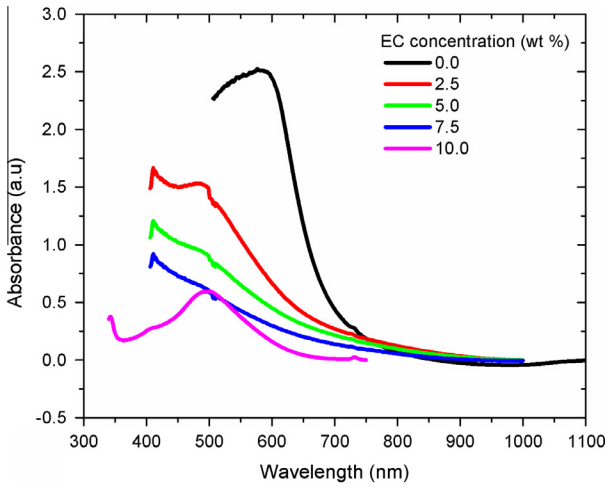

Fig. 4 Optical absorption spectra against wavelenght for colloidal for 10 wt.% CuI/PVA polymer composite blended with different concentrations of EC.

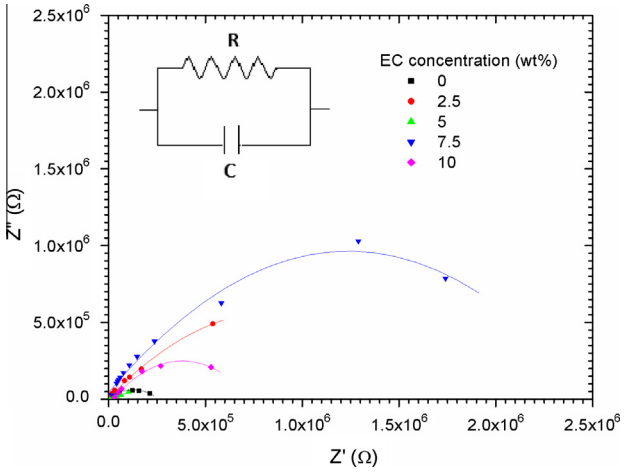

Fig. 5 Impedance plots (Cole–Cole plot) for 10 wt.% CuI/PVA polymer composite blended with different concentrations of EC.

band gap. Fig. 4 illustrates the plot of the optical absorption against wavelength in the visible range for polymer/CuI composites in colloidal having different concentrations of EC. It represents that the absorption peak position is affected with varying the concentration of EC, which shows a blue shift with the increasing EC concentration. In addition, the absorption edge varies also with increasing the concentration of EC in the PVA/CuI polymer composite. The optical band gap can be estimated from the following relationship [28–32];

$$(\alpha h\upsilon)^{1/n} = A(h\upsilon - E_g) \tag{2}$$

where A is constant, E_g is the optical band gap energy, $h\upsilon$ is the incident photon energy, α is the absorption coefficient, and the exponent n depends on the type of transition. $n = 1/2$, 2, 3/2, and 3 corresponding to allowed direct, allowed indirect, forbidden direct and forbidden indirect transitions, respectively. The appropriate transition has been tested by estimating the power n which predicts direct transition for PVA polymer composites under investigation. However, the optical band gap has been calculated by plotting $(\alpha h\upsilon)^2$ versus $h\upsilon$ and extrapolating the straight line portion of curve to intercept the energy axis in Eq. (2). The values of E_g are obtained for direct transition of the colloidal samples and listed in Table 1. It increases for direct transition from 1.7 to 2.18 eV as the EC increases up to 10 wt.%. It is evident that this can be attributed to the expected partial dissociation of CuI due to the decrease of polymer composite viscosity by EC plasticization. In addition, the observed increase of the band gap means a blue shift which can be attributed to the EC capping effect on CuI nanoparticles embedded in the PVA polymer. This blue shift resulted from the core–shell of CuI–EC, which exhibited plasmon–exciton interaction.

AC spectroscopy

Fig. 5, illustrates the impedance plot of the imaginary part Z'' against the real part Z', for polymer composite at room temperature as a representative diagram. The plot, in general, shows an arc (semicircle), its center below the Z' axis; the intersection with Z' axis, represents the sample bulk resistance, R_b. The values of bulk conductivity of the polymer composites were obtained from $\sigma_b = d/R_bA$, where d is the film thickness and A is its effective area for different concentrations of EC in the polymer composite [33]. Fig. 6 illustrates the temperature dependence of bulk conductivity of against EC concentration. It shows that the conductivity has been enhanced with increasing temperature. This indicates that the composites have been thermally activated, which can be explained on the way that the ions 'jump' into the neighboring vacant sites and cause an increase in the conductivity. The behavior which can be described by the following Arrhenius relation [34,35];

$$\sigma_b T = \sigma_{b0} \exp(-E_b/kT) \tag{3}$$

where E_b is the bulk conductivity activation energy. The values of E_b are obtained by the least square fitting and listed in Table 1 and lie within the range 0.21–0.97 eV. In general, E_b decreases with increasing EC content in the polymer composite. The higher value of the bulk conductivity 1×10^{-5} s/cm is

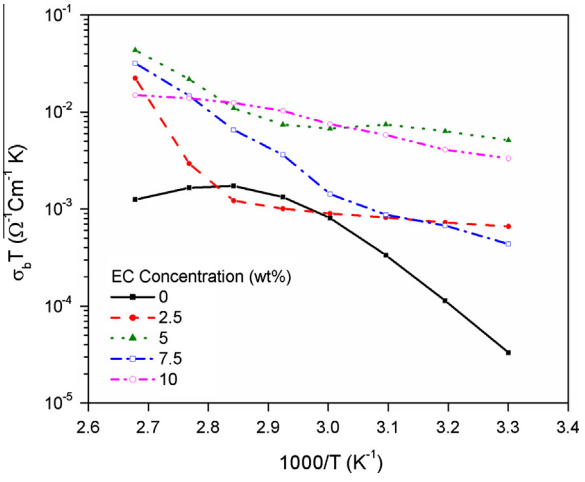

Fig. 6 Temperature dependence of bulk conductivity σ_b for 10% CuI/PVA polymer composite blended with different concentrations of EC.

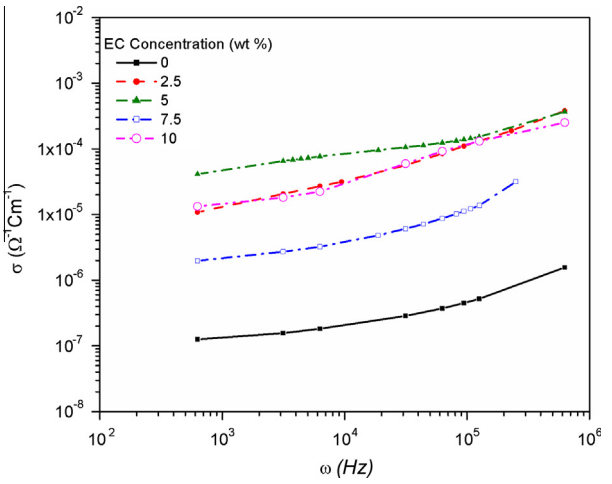

Fig. 7 Frequency dependence of total conductivity for 10% CuI/PVA polymer composite blended with different concentrations of EC.

obtained for 5 wt.% of EC. The reduction of E_b and increase in conductivity reflect the increase of charge carrier concentration besides facilitating charge carrier transportation of the host polymer composite (plasticization of polymer composite matrix).

In Fig. 7 the frequency dependence of the total conductivity in the polymer composite is shown at 303 K for the different values of EC concentration, which follow the universal power law [36];

$$\sigma_{ac}(\omega) = \sigma_{dc} + A\omega^{S} \tag{4}$$

where σ_{dc} is the *dc* conductivity (the extrapolation of the plateau region to zero frequency), A is the frequency independent pre-exponential factor, ω is the angular frequency and s is the frequency exponent. The values of the exponent S have been obtained using the least square fitting of Eq. (4) are listed in Table 1. The values of S lie within the range of $0.5 < S < 1$ for different concentration of EC except 2.5 wt.% concentration. It is equal to 0.29. In general, the values of s, predicts the domination of hopping conduction in CuI/PVA polymer composite matrix [37].

Dielectric properties

Fig. 8a and b show the variation of the dielectric permittivity ε' and dielectric loss ε'' versus frequency respectively at room temperature of 300 K. It is found that, both ε' and imaginary ε'' decrease monotonically with increasing frequency at $\omega\tau \gg 1$. This behavior can be described by the Debye dispersion relations [38];

$$\varepsilon' \cong \varepsilon_{\infty} + \frac{\varepsilon_s - \varepsilon_{\infty}}{1+\omega^2\tau^2}; \quad \varepsilon'' \equiv \frac{(\varepsilon_s - \varepsilon_{\infty})\omega\tau}{1+\omega^2\tau^2} \tag{5}$$

where ε_{∞} and ε_s are the static and infinite dielectric permittivity, τ is the relaxation time and ω is the angular frequency. This can be understood on the following, the decrease of ε' and ε'' with frequency can be associated with the inability of dipoles to rotate rapidly leading to a lag between frequency of oscillating dipole and that of applied field. The variation indicates that at low frequencies, the dielectric constant is high due to

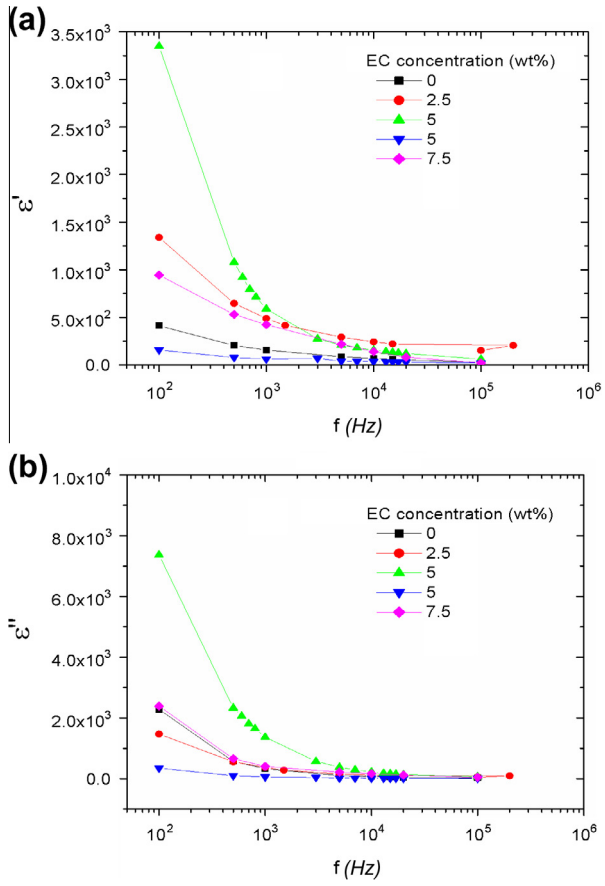

Fig. 8 Variation of (a) dielectric constant ε' and (b) dielectric loss ε'' with frequency for 10% CuI/PVA polymer composite blended with different concentrations of at 303 K.

the interfacial polarization. Moreover, the dielectric loss (ε'') becomes very large at lower frequencies due to free charge motion within the material [38]. On the other hand, the increase in the values of both ε' and ε'' at low frequency can be attributed to the interfacial polarization [39]. The larger value of dielectric loss at low frequency could be due to the existence of mobile charges within the polymer backbone besides the interfacial polarization at CuI and PVA interfaces. The values of both ε' and ε'' promote to maximum value at 5 wt.% (Table 2) which can be understood in terms of electrical conductivity that is associated with the dielectric loss in the presence of EC in the polymer composites under investigation. The PVA itself exhibits flexible side groups with polar bond as the bond rotating having an intense dielectric α-transition. Thus, there is a chemical composition change of the polymer repeated unit due to the formation of hydrogen bonds with hydroxyl groups through the polymerization process, which in turn makes the polymer chain flexible and hence enhances the electrical conductivity [40]. Fig. 9a and b show the variation of the dielectric constant ε' and dielectric loss ε'' versus temperature T, at frequency of 1 kHz. It can be seen from these figures that both ε' and ε'' increases with increasing temperature up to asymptotic value nearly at the T_g. Both the ε' and ε'' show temperature dependence for CuI/PVA without EC and obey well Debye equations where a peak in dielectric loss appeared at relatively higher temperature range. The values of both ε'

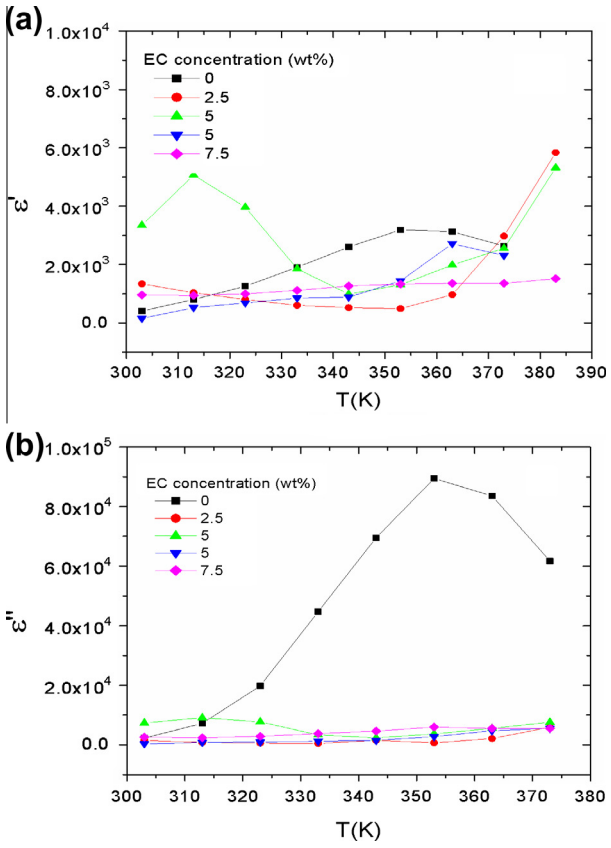

Fig. 9 Variation of (a) dielectric constant ε' and (b) dielectric loss ε'' with frequency for 10% CuI/PVA polymer composite blended with different concentrations of at 100 Hz.

and ε'' have been suppressed by the addition of EC to CuI/PVA polymer composite. This general behavior of ε' and ε'' is typical of polar dielectrics in which the orientation of dipoles is facilitated with the rising temperatures which are rigidly fixed at a lower temperature, therefore, respond to the applied electric field. Thus, due to the increase in polarization the dielectric constant is also increased [41].

Conclusion

The study of 10 wt.% CuI/PVA polymer composite blended with different concentrations of EC shows significant effect of structure, thermal stability, electrical conductivity, dielectrical relaxation and optical absorption. Both T_g and T_m shows small increase with increasing EC indicates the thermal stability of the polymer composite matrix. The conductivity of 10 wt.% CuI/PVA polymer composite increased by two orders of magnitude from 1×10^{-7} to 1×10^{-5} S/cm with the reduction in activation energy from 0.79 to 0.21 eV with the addition of EC. Subsequently the optical absorption shows a blue shift towards the intensive region of solar spectra in the visible range.

Conflict of interest

The authors have declared no conflict of interest.

Acknowledgement

This project was supported financially by the Science and Technology Development Fund (STDF), Egypt, Grant No: 1360.

References

[1] Günes S, Sariciftci NS. Hybrid solar cell. Inorg Chim Acta 2008;361(3):581–8.
[2] Kim S, Chung DS, Cha H, Jang JW, Kim Y, Kang J, et al. Thermally stable organic bulk heterojunction photovoltaic cells incorporating an amorphous fullerene derivative as an electron acceptor. Sol Energy Mater Sol Cells 2011;95(2):432–9.
[3] Peumans P, Uchida S, Forrest SR. Efficient bulk heterojunctio photovoltaic cells using small molecular-weight organic thin films. Nature 2003;425(6954):158–62.
[4] Scharber MC, Mühlbacher D, Koppe M, Denk P, Waldauf C, Heeger AJ, et al. Design rules for donors in bulk-heterojunction solar cells – towards 10% energy-conversion efficiency. Adv Mater 2006;18(6):789–94.
[5] Deibel C, Dyakonov V, Brabec CJ. Organic bulk-heterojunction solar cells. IEEE J Sel Top Quant 2010;16(6):1517–27.
[6] Tawansi A, El-Khodary A, Abdelnaby MM. A study of the physical properties of FeCl3 filled PVA. Curr Appl Phys 2005;5(6):572–8.
[7] Wang H, Fang P, Chen Z, Wang S. Synthesis and characterization of CdS/PVA nanocomposite films. Appl Surf Sci 2007;253(20):8495–9.
[8] Wang H, Fang P, Chen Z, Shaojie Wang. Structural and optical characterization of CdS nanorods synthesized by a PVA-assisted solvothermal method. J Alloys Compd 2008;461(1–2):418–22.
[9] Xu J, Cui X, Zhang J, Liang H, Wang H, Li J. Preparation of CuS nanoparticles embedded in poly (vinyl alcohol) nanofibre via electrospinning. Bull Mater Sci 2008;31(2):189–92.
[10] Bouhafs B, Heireche H, Sekkal W, Aourag H, Certier M. Electronic and optical properties of copper halides mixed crystal $CuCl_{1-x}I_x$. Phys Lett A 1998;240(4–5):257–64.
[11] Kumarasinghe AR, Flavell WR, Thomas AG, Mallick AK, Tsoutsou D, Chatwin C, et al. Electronic properties of the interface between *p*-CuI and anatase-phase *n*-TiO2 single crystal and nanoparticulate surfaces: a photoemission study. J Chem Phys 2007;127(114703):1–14.
[12] Sekkal W, Zaoui A. Monte carlo study of transport properties in copper halides. Physica B 2002;315(1–3):201–9.
[13] Amalina MN, Azman MA, Noor UM, Mahmood MR. Comparison on the electrical, structural and optical properties of CuI thin films deposited by spin coating and by atomization method. Adv Mater Res 2012;403–408:451–5.
[14] Qi L, Co1lfen H, Antonietti M. Synthesis and characterization of CdS nanoparticles stabilized by double hydrophilic block copolymers. Nano Lett 2001;1(2):61–5.
[15] Kim JY, Koo HM, Ihn KJ, Suh KD. Synthesis of CdS nanoparticles dispersed within solutions and polymer films using amphiphilic urethane acrylate chains. J Ind Eng Chem 2009;15(1):103–9.
[16] Rajendran S, Sivakumar M, Subadevi R. Investigations on the effect of various plasticizers in PVA–PMMA solid polymer blend electrolytes. Mater Lett 2004;58(5):641–9.
[17] Ram S, Mandal TK. Photoluminescence in small isotactic, atactic and syndiotactic PVA polymer molecules in water. Chem Phys 2004;303(1–2):121–8.
[18] Pitawala HMJC, Dissanayake MAKL, Seneviratne VA, Mellander BE, Albinson I. Effect of plasticizers (EC or PC) on the ionic conductivity and thermal properties of the $(PEO)_9$ LiTf: Al_2O_3 nanocomposite polymer electrolyte system. J Solid State Electrochem 2008;12(7):783–9.

[19] Rahman MYA, Ahmad A, Lee TK, Farina Y, Dahlan HM. Effect of ethylene carbonate (EC) plasticizer on poly (Vinyl Chloride)-liquid 50% epoxidise natural rubber (LENR50) based polymer electrolyte. Mater Sci Appl 2011;2(7):818–26.
[20] Sharma GD, Shanap TS, Patel KR, El-Mansy MK. Photovoltaic properties of bulk heterojunction devices based CuI–PVA as electron donor and PCBM and modified PCBM as electron acceptor. Mater Sci Poland 2012;30(1):10–6.
[21] El-Mansy MK, Sheha EM, Patel KR, Sharma GD. Characterization of PVA/CuI polymer composites as electron donor for photovoltaic application. Optik 2013;124(13):1624–1631.
[22] Makled MH, Sheha E, Saleh T, El-Mansy MK. Electrical conduction and dielectric relaxation in *P*-type PVA/CuI polymer composite. J Adv Res 2013;4(6):531–538.
[23] Mooney RCL. An X-ray study of the structure of polyvinyl alcohol. J Am Chem Soc 1941;63(10):2828–32.
[24] Rajendran S, Sivakumar M, Subadevi R. Li-ion conduction of plasticized PVA solid polymer electrolytes complexed with various lithium salts. Solid State Ionics 2004;167(3–4):335–9.
[25] Badr Y, Mahmoud MA. Effect of PVA surrounding medium on ZnSe nanoparticles: size, optical, and electrical properties. Spectrochim Acta Part A 2006;65(3–4):584–90.
[26] Agrawal SL, Awadhia A. DSC and conductivity studies on PVA based proton conducting gel electrolyte. Bull Mater Sci 2004;27(6):523–7.
[27] Peppas NA, Merrill EW. Deferential scanning calorimetry of crystallized PVA hydrogels. J App polym Sci 1976;20(6):1457–65.
[28] Osuwa JC, Oriaku CI, Ezema FI. Impurity effects of cadmium salt on the absorption edge and structure of chemically prepared PbS films. Chalcogenide Lett 2009;6(8):385–91.
[29] Asogwa PU. Band gap shift and optical characterization of PVA-capped PbO thin films: effect of thermal annealing. Chalcogenide Lett 2011;8(3):163–70.
[30] Osuwa JC, Oriaku CI, Kalu IA. Variation of optical band gap with post deposition annealing in CdS/PVA thin films. Chalcogenide Lett 2009;6(9):433–6.
[31] Borah JP, Sarma KC. Optical and optoelectronic properties of ZnS nanostructured thin film. Acta Phys Pol A 2008;114(4):713–9.
[32] Osuwa JC, Uwaezi PU. Effect of annealing on optical and solid state properties of NiS_2 thin films. Chalcogenide Lett 2011;8(9):587–94.
[33] Mohan VM, Qiu W, Shen J, Chen W. Electrical properties of poly(vinyl alcohol) (PVA) based on $LiFePO_4$ complex polymer electrolyte films. J Polym Res 2010;17(1):143–50.
[34] Austin IG, Mott NF. Polaron in crystalline and non crystalline materials. Adv Phys 1969;18(71):41–102.
[35] Mondal SP, Aluguri R, Ray SK. Dielectric and transport properties of carbon nanotube-CdS nanostructures embedded in polyvinyl alcohol matrix. J Appl Phys 2009;105(11):114317–23.
[36] Harun MH, Saion E, Kassim A, Hussain MY, Mustafa IS, Omer MAA. Temperature dependence of ac electrical conductivity of PVA-PPy-$FeCl_3$ composite polymer films. Malays Polym J (MPJ) 2008;3(2):24–30.
[37] Abd El-kader FH, Osman WH, Mahmoud KH, Basha MAF. Dielectric investigations and ac conductivity of polyvinyl alcohol films doped with europium and terbium chloride. Physica B 2008;403(19):3473–84.
[38] Sheha E, Khoder H, Shanap TS, El-Shaarawy MG, El Mansy MK. Structure, dielectric and optical properties of P-type (PVA/CuI) nanocomposite polymer electrolyte for photovoltaic cells. Optik 2012;123(13):1161–6.
[39] Dutta P, Biswas S, De SK. Dielectric relaxation in polyaniline–polyvinyl alcohol composites. Mater Res Bull 2002;37(1):193–200.
[40] Harun MH, Saion E, Kassim A, Mahmud E, Hussain MY, Mustafa IS. Dielectric properties of poly (vinyl alcohol)/polypyrrole composite polymer films. J Adv Sci Arts 2009;1(1):9–16.
[41] Akram M, Javed A, Rizvi TZ. Dielectric properties of industrial polymer composite materials. Turk J Phys 2005;29(6):355–62.